



HAL
open science

Gain sideband splitting in dispersion oscillating fibers

Christophe Finot, Stefan Wabnitz

► **To cite this version:**

Christophe Finot, Stefan Wabnitz. Gain sideband splitting in dispersion oscillating fibers. NonLinear Photonics, Jul 2014, Barcelona, Spain. pp.JTu3A.17. hal-01001729

HAL Id: hal-01001729

<https://hal.science/hal-01001729v1>

Submitted on 2 Aug 2014

HAL is a multi-disciplinary open access archive for the deposit and dissemination of scientific research documents, whether they are published or not. The documents may come from teaching and research institutions in France or abroad, or from public or private research centers.

L'archive ouverte pluridisciplinaire **HAL**, est destinée au dépôt et à la diffusion de documents scientifiques de niveau recherche, publiés ou non, émanant des établissements d'enseignement et de recherche français ou étrangers, des laboratoires publics ou privés.

Gain sideband splitting in dispersion oscillating fibers

Christophe Finot^{1,*} and Stefan Wabnitz²

¹Laboratoire Interdisciplinaire Carnot de Bourgogne (ICB), UMR 6303 CNRS/Université de Bourgogne, Dijon, France

²Department of Information Engineering, Università di Brescia, Brescia, Italy

* christophe.finot@u-bourgogne.fr

Abstract: We analyze the modulation instability spectrum in a varying dispersion optical fiber as a function of the dispersion oscillation amplitude, and predict a novel sideband splitting into different sub-sidebands for relatively large dispersion oscillations.

OCIS codes: (060.4370) Nonlinear optics, fibers; (190.4380) Nonlinear optics, four-wave mixing;

1. Introduction

Modulation instability (MI) has been widely investigated in various fields of physics, e.g., plasma, hydrodynamics and optics. MI leads to the emergence and amplification of gain sidebands in the spectrum of an initially intense continuous wave. MI has been demonstrated in fibers with anomalous group-velocity dispersion (GVD), and in normal dispersion fibers with fourth order dispersion, birefringence or multimode coupling. More recently, renewed experimental and theoretical interest in the MI process has been stimulated by using fibers with a longitudinal and periodic modulation of the GVD [1]. Indeed, thanks to parametric resonance induced by the periodic variation of GVD, scalar MI sidebands can emerge even in the normal average GVD regime of a dispersion-oscillating fiber (DOF) [2]. Recent experiments confirmed resonant MI in microstructure DOF around 1 μm [1], and in non-microstructure, highly nonlinear DOF at telecom wavelengths [3].

So far, the role of the amplitude of GVD oscillations has been largely overlooked. In this contribution, we present a systematic study of the various sidebands which are numerically observed at the output of a DOF as the amplitude of the dispersion variations grows larger. We unveil the emergence of new sidebands as well as their splitting in sub-sidebands. We are able to provide an analytical description of these effects based on the formalism of [1].

2. Situation under investigation

We numerically consider the evolution of a cw with an average power of 0.75 W in an optical single-mode optical fiber with a longitudinal periodic variation of its GVD. The evolution of the optical field can be described by the nonlinear Schrödinger equation that includes both Kerr nonlinearity γ and a second-order GVD $\beta_2(z)$ which varies with distance according to $\beta_2(z) = \beta_{2av} + \beta_{2amp} \sin(2\pi z/\Lambda)$, with β_{2av} , β_{2amp} and Λ being the average dispersion, the amplitude of the dispersion variation and the spatial period respectively. We consider here a fiber with $\gamma = 2$ /W/km, $\Lambda = 1$ km and $\beta_{2av} = -0.5$ ps/km/nm.

In this situation, MI gives rise to quasi-phase-matched (QPM) sidebands, whose central frequency Ω_p and gain G_p after a propagation length L can be analytically predicted by the formulas [1, 2]

$$\Omega_p = \pm \sqrt{\frac{2\pi p / \Lambda - 2\gamma P}{\beta_{2av}}} \quad \text{and} \quad G_p = \exp \left[2\gamma P L \left| J_p \left(\frac{\beta_{2amp} \Omega_p^2}{2\pi / \Lambda} \right) \right| \right] \quad (1)$$

where $p = 1, 2, 3 \dots$ is the QPM sideband order, and J_p is the Bessel function of order p .

3. Influence of the amplitude of dispersion fluctuation

We investigate the influence of the amplitude of dispersion fluctuations β_{2amp} on the spectrum recorded after 12 spatial periods. Results are summarized in Fig. 1(a): as can be seen, the output spectrum and the detailed structure of the MI sidebands exhibit significant changes as the amplitude of GVD oscillations grows larger.

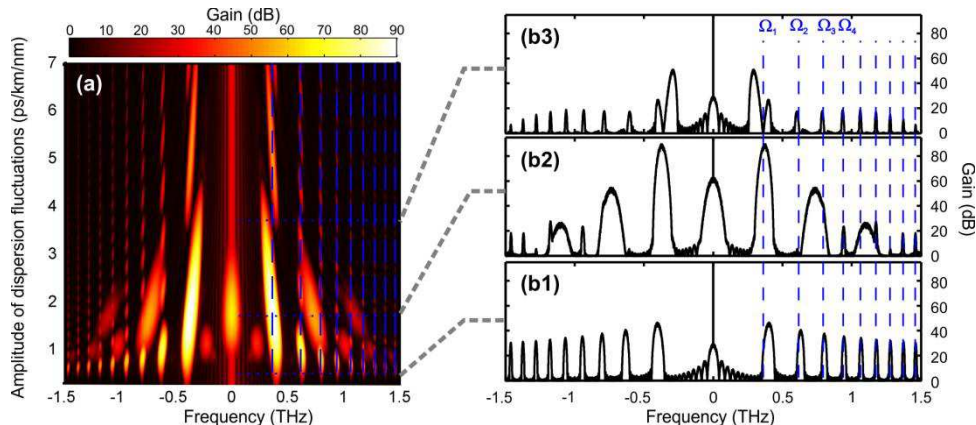


Fig. 1. (a) Evolution of the output spectra according to the amplitude of the dispersion fluctuation. (b) Details of the spectra for $\beta_{2amp} = 0.5$ ps/km/nm, 1.7 ps/km/nm and 3.7 ps/km/nm. Vertical dashed lines represent the predictions from Eq. (1).

For a 0.5 ps/km/nm (subplot b1) GVD oscillation amplitude, we observe the generation of a set of unequally spaced and narrow spectral sidebands whose positions are in qualitative agreement with the analytical predictions of Eq. (1) (see dashed vertical lines). For increasing GVD oscillation amplitudes (1.7 ps/km/nm, subplot b2), we first notice that some spectral lines (for example lines corresponding to $p = 2$ or $p = 5$) have disappeared, in agreement with Eq. 1 [1]. To the opposite, we also point out the development of a set of regularly spaced sidebands with a broader bandwidth. This feature is linked to four wave mixing between the pump wave and the first QPM sideband and further cascading of the process, as experimentally demonstrated in [3].

For an even higher dispersion oscillation amplitude, e.g., 3.7 ps/km/nm (subplot b3), we observe instead of a single gain sideband, the unexpected emergence of a pair of sidebands around the frequency Ω_j . As our model is scalar and it does not take into account higher order terms of dispersion, these new sidebands cannot be linked to fourth-order dispersion induced MI or to vectorial four-wave mixing processes. We have also checked these new sidebands cannot be explained through the mixing between the various other bands.

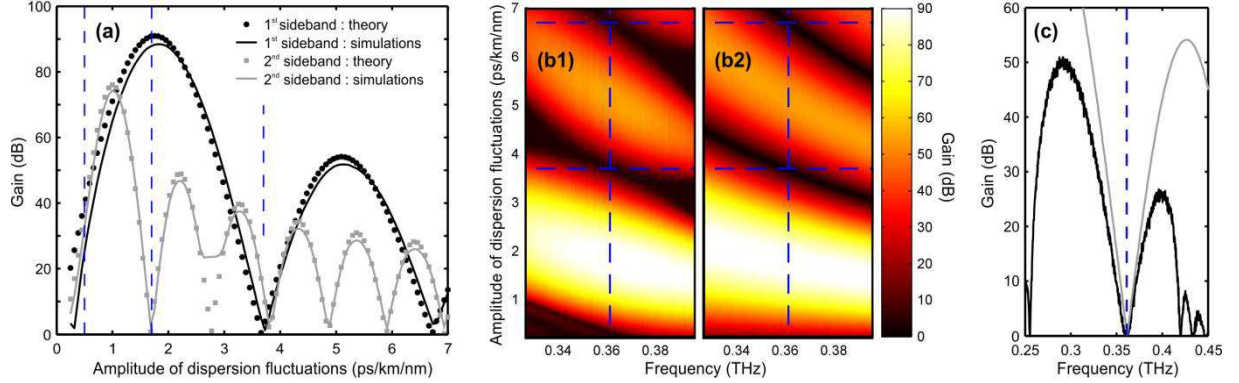


Fig. 2. (a) Evolution of MI gain at the wavelength predicted by Eq. (1) for the first and second QPM sidebands. (b) Magnification of the spectral region around Ω_j according to the amplitude of the dispersion fluctuations. Numerical results (b1) are compared with analytical results (b2) predicted by Eq. (2). Blue dashed vertical lines indicate the frequency Ω_j . (c) Output spectrum for $\beta_{2amp} = 3.7$ ps/km/nm obtained from numerical simulations (black line) and from Eq. (2) (grey line).

We have studied more precisely the evolution of the gain occurring at the wavelengths predicted by Eq. (1). The corresponding results are summarized on Fig 2(a), and demonstrate an excellent agreement between the analytical predictions of Eq. (1) with the gain evaluated from numerical simulations for Ω_1 and Ω_2 . The most important conclusion here is that the observation of two sidebands either side of the frequency Ω_1 in Fig 1b3 does not question the validity of the analytical predictions of Eq. (1).

In order to better understand the emergence of the two neighboring sidebands, we have plotted a magnification of the first QPM sideband as obtained from numerical simulations (see Fig. 2(b1)), that we may compare with the following analytical expression (Fig 2(b2)), which is an extension of Eq. 1, that was originally aimed at describing the gain at the QPM frequency only

$$G(\omega) = \exp \left[2\gamma P L \left| J_1 \left(\frac{\beta_{2amp} \omega^2}{2\pi / \Lambda} \right) \right| \right] \quad (2)$$

As shown in panel 2(b2), we can see that Eq. 2 provides an interesting insight in the existence of the two sidebands from either side of the wavelength Ω_j : despite the use of Eq. 2 is not strictly rigorous, it qualitatively reproduces the structure of the first MI band. Indeed, as also illustrated in subplot 2(c), which compares the structure of the gain around Ω_j , the analytical expression (2) reproduces the inner slope of the two sidebands.

4. Conclusion

We predicted the splitting of QPM MI sidebands into two sub-sidebands in a DOF with large-amplitude dispersion oscillations. The existence of these two sidebands does not violate existing analytical predictions, and a link can be made with the parameters leading to an expected vanishing gain at the central resonant sideband frequency. The two sub-sidebands that emerge in the vicinity of the central QPM frequency can be qualitatively well reproduced by extending the analytical discrete resonant gain spectrum into a continuum of frequencies.

5. References

1. M. Droques, A. Kudlinski, G. Bouwmans, G. Martinelli, and A. Mussot, "Dynamics of the modulation instability spectrum in optical fibers with oscillating dispersion," *Phys. Rev. A* **87**, 013813 (2013).
2. N. J. Smith and N. J. Doran, "Modulational instabilities in fibers with periodic dispersion management," *Opt. Lett.* **21**, 570 (1996).
3. C. Finot, J. Fatome, A. Sysoliatin, A. Kosolapov, and S. Wabnitz, "Competing four-wave mixing processes in dispersion oscillating telecom fiber," *Opt. Lett.* **38**, 5361-5364 (2013).